



## Optimization of anti-MRSA compound production by *Streptomyces* sp. AR05 using an integrated RSM-ANN-GA approach

Fateh Merouane<sup>1\*</sup>; Amani Kifadji<sup>2</sup>; Racha Mansouri<sup>3</sup>; Meroua Safa Mechouche<sup>1,4</sup>; Chemes El-Houda Messaad<sup>5,6</sup>; Anfal Bellebcir<sup>1</sup>

<sup>1</sup>Biotechnology Laboratory, Higher National School of Biotechnology Taoufik KHAZNADAR, Constantine-3 University, Ali Mendjeli, 25100 Constantine, Algeria; <sup>2</sup>Laboratory of Plant Biology and Environment, Faculty of Sciences, Badji Mokhtar University. 23000 Annaba, Algeria; <sup>3</sup>Faculty of Medicine, Paris-Saclay University, 91190 Paris, France; <sup>4</sup>University Lille, CNRS, University Polytechnique Hauts-de-France, UMR 8520, IEMN, F-59000, Lille, France; <sup>5</sup>Laboratory of Applied Microbiology, Faculty of Sciences of Nature and Life, Ferhat Abbas University. 19000 Setif, Algeria; <sup>6</sup>Laboratory of Biodiversity and Biotechnological Technics for the Valuation of Plant Resources (BTB-VRV), Faculty of Sciences, SNV Department, Mohamed Boudiaf University, 28000 M'sila, Algeria

\*Corresponding author E-mail: [f.merouan@ensbiotech.edu.dz](mailto:f.merouan@ensbiotech.edu.dz)



Received: 4 August, 2024; Accepted: 8 September, 2024; Published online: 9 September, 2024

### Abstract

The emergence of multidrug-resistant pathogens, such as methicillin-resistant *Staphylococcus aureus* (MRSA), poses a significant threat to the global public health. *Streptomyces* species have been recognized as a prolific source of bioactive secondary metabolites, including antimicrobial compounds. In this study, we aimed to optimize the production of anti-MRSA compounds by *Streptomyces* sp. AR05; a strain isolated from hydrocarbon-contaminated soil, using an integrated approach combining response surface methodology (RSM), artificial neural networks (ANN), and genetic algorithms (GA). The strain was identified through 16S rRNA gene sequencing and exhibited significant genetic similarity to *Streptomyces kurssanovii* and *Streptomyces ostreogriseus*. Using the Plackett-Burman design, the most important variables affecting the anti-MRSA activity were found to be peptone, CaCO<sub>3</sub>, and pH. These factors were optimized using Box-Behnken design, while RSM and ANN were utilized for modeling the experimental data. The predicted accuracy of ANN model was higher than that of the RSM model, with lower values of mean absolute percentage error (MAPE) and root mean square error (RMSE). Sensitivity analysis of the ANN model identified peptone as the most influential factor, followed by pH and CaCO<sub>3</sub>. The ANN model was further optimized using GA, and the optimized conditions (5.34 g/l peptone, 1.54 g/l CaCO<sub>3</sub>, pH 6.07) were experimentally validated, resulting in a 48.87 % increase in anti-MRSA activity compared to the initial conditions. The developed RSM-ANN-GA



### Copyright policy

NRMJ allows the author(s) to hold the copyright, and to retain publishing rights without any restrictions. This work is licensed under the terms and conditions of the Creative Commons Attribution (CC BY) license (<https://creativecommons.org/licenses/by/4.0/>)

approach demonstrated the potential for enhancing the production of valuable antibacterial compounds from *Streptomyces* species and contributed to the global efforts to combat antimicrobial resistance.

**Keywords:** *Streptomyces* sp. AR05, Anti-MRSA compounds, Response surface methodology, Artificial neural network, Genetic algorithm, Optimization

## 1. Introduction

Antibacterial resistance has emerged as a global public health challenge, with the development of new antibiotics lagging behind the increasing prevalence of multidrug-resistant pathogens ([Lertcanawanichakul and Chawawisit, 2019](#)). Methicillin-resistant *Staphylococcus aureus* (MRSA) is one such 'superbug' that poses a significant threat to healthcare systems worldwide, causing a wide range of nosocomial infections associated with increased morbidity, mortality, and healthcare costs ([Kemung \*et al.\*, 2018](#); [Sharma and Manhas, 2019](#)). The intrinsic tendency of traditional antibiotics to exert selective pressure on bacterial populations, coupled with their inappropriate and excessive utilization, has played a significant role in the emergence of multidrug-resistant pathogens, underscoring the pressing need for the identification and development of innovative antimicrobial agents ([de Lima Procópio \*et al.\*, 2012](#)).

The *Streptomyces* genus has emerged as a prominent reservoir of bioactive secondary metabolites, demonstrating the capacity to generate an extensive range of compounds possessing antibacterial, antifungal, antiviral, and antitumor activities, which has become a focal point of scientific investigations ([Kemung \*et al.\*, 2018](#); [Sharma and Manhas, 2019](#)). Extensive researches have been conducted on these filamentous prokaryotes for a period exceeding eight decades for their incredible array of specialized metabolites ([Martinet \*et al.\*, 2023](#)). The remarkable metabolic diversity of *Streptomyces* spp. has made them a primary target to find new antibacterial substances that can combat the rising threat of antibiotic resistance ([Bhakyashree and Kannabiran, 2020](#)). While *Streptomyces* spp. are

ubiquitous in soil environments, those inhabiting extreme or under explored habitats have emerged as promising sources of novel antimicrobial agents, including several compounds active against MRSA.

Exploring the underexploited and extreme environments such as polluted habitats, has gained increasing interest as a strategy for uncovering new *Streptomyces* strains capable of producing novel anti-MRSA compounds ([Shivlata and Satyanarayana, 2015](#)). Contaminated environments, including soils and sediments polluted with heavy metals, hydrocarbons, or pesticides, pose a selective stress on the microbial communities, driving them toward the evolution of unique metabolic pathways and cryptic biosynthesis gene clusters' activation ([Tormo \*et al.\*, 2003](#)). Moreover, the intense competition for limited nutritional resources in these ecological niches may prompt the actinobacteria to produce antimicrobial secondary metabolites to gain a selective advantage ([Antoraz \*et al.\*, 2015](#)). Notable examples were those *Streptomyces* spp. isolated from various soil contaminated with petroleum in Kurdistan, which displayed antibacterial activity against human pathogens such as *Escherichia coli* and *Staphylococcus aureus* ([Jalal and Hasan, 2021](#)). Similarly, *Streptomyces* strains from petroleum-contaminated soils demonstrated the ability to degrade hydrocarbons and produce antibiotics, attributable to the development of mutations within the gene for RNA polymerase  $\beta$ -subunit (*rpoB*) ([Rachid, 2012](#)). Another strain isolated from contaminated soil; *S. coeruleorubidus* MO11, has shown strong inhibitory activity against *Pantoea calida*, an opportunistic pathogen ([Aburas, 2022](#)). These findings underscore

the potentials of *Streptomyces* spp. from contaminated and underexplored niches as sources of novel anti-MRSA compounds.

Optimization of fermentation conditions and media composition plays a crucial role in maximizing the production of bioactive metabolites by *Streptomyces* spp. (Kumar *et al.*, 2017). Response surface methodology (RSM) and artificial neural networks (ANN) have proven to be powerful tools for modeling and optimizing complex bioprocesses, enabling researchers to identify optimal conditions for enhanced antibiotic production (Lau *et al.*, 2023). The integration of these statistical and machine learning approaches with genetic algorithms (GA) has further improved the efficiency and effectiveness of bioprocess optimization strategies (Alloun *et al.*, 2023).

The objective of the present study was to optimize the production of anti-MRSA compounds by *Streptomyces* sp. AR05 strain using an integrated RSM-ANN-GA approach. By leveraging the strengths of statistical modeling, machine learning, and global optimization techniques, we seek to develop a comprehensive and effective strategy to enhance the antimicrobial potential of this promising strain. Successful optimization of anti-MRSA compounds production by *Streptomyces* sp. AR05 could contribute to the global efforts to combat antimicrobial resistance and enhance the pace of uncovering and formulating new antibacterial compounds that can tackle the mounting issue of microorganisms exhibiting resistance to various medications.

## 2. Material and methods

### 2.1. Isolation and maintenance of *Actinobacteria* strain AR05

The actinobacteria strain AR05 was isolated from a hydrocarbon-contaminated soil at the SPA NAFTAL site in Bounouara, Constantine, Algeria (Mechouche *et al.*, 2022). Following an evaluation of multiple actinomycete isolates, this strain was selected owing to its capacity to generate antibiotics displaying

inhibitory effects on the development of Gram-positive and Gram-negative bacterial pathogens. AR05 was cultured and maintained on the International Streptomyces Project medium N°2 (ISP 2): glucose (4 g/l), malt extract (10 g/l), yeast extract (4 g/l) and agar (20 g/l) in dist. water, with pH adjusted to 7.2 (Atlas, 2010).

### 2.2. Molecular identification

The 16S rRNA gene sequencing technique was employed to establish the molecular identity of isolate AR05. The extraction of genomic DNA was carried out according to the protocol outlined by Hopwood, (1985). Universal primers 16S-27F and 16S-1492R were used to amplify the entire 16S rRNA gene through polymerase chain reaction (PCR), with suitable controls incorporated. The PCR was performed in a 30 µl reaction volume containing 2 µl genomic DNA, 1 µl of each primer, 6 µl 5X PCR Mix, and 20 µl H<sub>2</sub>O to reach a final volume of 30 µl. The reaction was initiated by activating the Hot-Start Mix at 96 °C for 12 min, followed by 35 cycles of denaturation at 96 °C for 20 sec, annealing at 56 °C for 20 sec, and extension at 72 °C for 30 sec. A final extension step was carried out at 72 °C for 5 min. The PCR product was validated using high-resolution capillary electrophoresis, purified, and sequenced using internal primers. The resulting sequence data were analyzed to construct a complete 16S gene contig, which was subsequently subjected to BLAST analysis for strain identification.

### 2.3. Selection of the best medium for anti-MRSA activity

To determine the optimal culture medium for anti-MRSA activity, strain AR05 was cultured on five different production media using the streak plate method (Dar and Ahmad, 2024). The media tested were: Bennett's medium: glucose (10 g/l), casamino acids (2 g/l), yeast extract (1 g/l), beef extract (1 g/l), agar (15 g/l), pH 7.0 (Goodfellow *et al.*, 1989); Czapek medium: sucrose (30 g/l), peptone (5 g/l), NaNO<sub>3</sub> (3 g/l), yeast extract (2 g/l), K<sub>2</sub>HPO<sub>4</sub> (1 g/l),

KCl (0.5 g/ l), MgSO<sub>4</sub>•7H<sub>2</sub>O (0.5 g/ l), FeSO<sub>4</sub>•7H<sub>2</sub>O (0.01 g/ l), agar (15 g/ l), pH 7.3 ([Thom and Raper, 1945](#)); Yeast Malt Agar (YMA) medium: malt extract (10 g/ l), glucose (4 g/ l), yeast extract (4 g/ l), CaCO<sub>3</sub> (2 g/ l), agar (20 g/ l), pH 7.2 ([Wickerhams, 1951](#)); Glycerol Bouillon Agar (GBA) medium: glycerol (20 g/ l), peptone (10 g/ l), meat extract (5 g/ l), CaCO<sub>3</sub> (3 g/ l), soluble starch (20 g/ l), agar (15 g/ l), pH 7.0 ([Shomura, 1979](#)); Starch Casein Agar (SCA) medium: Soluble starch (1 g/ l), K<sub>2</sub>HPO<sub>4</sub> (2 g/ l), KNO<sub>3</sub> (2 g/ l), NaCl (2 g/ l), casein (0.3 g/ l), MgSO<sub>4</sub>•7H<sub>2</sub>O (0.05 g/ l), CaCO<sub>3</sub> (0.02 g/ l), FeSO<sub>4</sub>•7H<sub>2</sub>O (0.05 g/ l), agar (15 g/ l), pH 7.5 ([Wellington and Cross, 1983](#)).

All culture media were poured into petri plates to achieve a 5 mm thickness of agar. Following inoculation of the AR05 strain using a dense streaking pattern, the plates were incubated for 10 d at 30 °C. Subsequent to incubation, growth was halted by exposing the plates to chloroform vapors in a sealed environment for 30 min. The agar cylinder method was used to assess the anti-MRSA potential of the cultures ([Evangelista-Martínez \*et al.\*, 2022](#)). The medium exhibiting the most potent antibacterial activity was selected for further optimization of its culture conditions using several statistical methods.

#### 2.4. Evaluation of anti-MRSA activity

MRSA strain (GenBank accession no: PKSS01000000) acquired from the bacteriology lab (CHU Constantine) was used as a reference strain to test the antibacterial activity. This pathogen was particularly resistant to β-lactam antibiotics and had acquired resistance to several other antibiotics, including fluoroquinolones, macrolides, lincosamides, and aminoglycosides.

A suspension of MRSA cells was made using physiological water (0.9 % NaCl) from an 18 h culture grown on nutrient agar (NA). The suspension's cell density was adjusted through dilution to attain an optical density at 620 nm between 0.08 and 0.1, equating to a final concentration of 10<sup>6</sup> cfu/ ml. Subsequently, a uniform volume of 0.1 ml bacterial

inoculum was applied and enseeded by swabbing to the Mueller Hinton (MH) agar plate surface. The plates were then left undisturbed until the medium had completely absorbed the bacterial suspension according to the Clinical and Laboratory Standards Institute's guidelines ([CLSI, 2023](#)). Inhibitory efficacy was evaluated using the agar-disk diffusion method as described by ([Evangelista-Martínez \*et al.\*, 2022](#)). Using a punch, 9 mm diameter agar cylinders were obtained from the AR05 strain plate, which were then placed on MH agar plate that had been previously inoculated with MRSA, followed by incubation at 37 °C for 24 h. Following incubation, a caliper was used to quantify the dimensions of the zones of inhibition.

#### 2.5. Statistical modeling

##### 2.5.1. Determination of key elements *via* Plackett-Burman screening methodology

Following selection of the optimal culture medium, a Plackett-Burman design (PBD) was used to analyze the factors most significantly influencing anti-MRSA activity ([Plackett and Burman, 1946](#)). The GBA culture medium components; mainly glycerol, starch, peptone, meat extract, CaCO<sub>3</sub> and pH were selected as factors for this study. To assess these six factors, twelve tests were carried out in triplicates (Table S1). Three further tests were conducted at the center points, and each variable was represented at two levels: high (+1) and low (-1) (Table 1). The Design-Expert software version 13 (Stat-Ease, Inc., MN, USA) was utilized to estimate the influence of each element and establishes its significance by the application of Student's t-test. Factors with confidence levels higher than 95 % were considered to play a crucial role in the production of inhibitory substances effective against MRSA and were therefore included in the optimization process.

##### 2.5.2. Box-Behnken design optimization

To gain a comprehensive understanding of the interactions among the different factors influencing the anti-MRSA activity of AR05 strain and to identify their optimal levels, a Box-Behnken experimental

**Table 1.** Actual values of the Plackett-Burman design screened independent variables

Factor	Name	Unit	Level	
			-1	+1
X <sub>a</sub>	Glycerol	g/l	10	30
X <sub>b</sub>	Starch	g/l	10	30
X <sub>c</sub>	Peptone	g/l	5	15
X <sub>d</sub>	Meat extract	g/l	2.5	7.5
X <sub>e</sub>	CaCO <sub>3</sub>	g/l	1.5	4.5
X <sub>f</sub>	pH	–	6	8

design (BBD) was used ([Box and Behnken, 1960](#)). Based on the results of a prior Plackett-Burman screening, three independent variables were selected: Peptone concentration (X<sub>1</sub>), CaCO<sub>3</sub> concentration (X<sub>2</sub>), and pH (X<sub>3</sub>). Each factor was investigated at three coded levels (Table 2). A total of 15 experiments, including 3 central points were conducted in triplicates; with each replicate considered as a separate block.

The Box-Behnken experimental design matrix and the corresponding anti-MRSA responses are presented in Table (3). Statistical examination of the experimental results was accomplished with the aid of a Design-Expert software version 13. (Stat-Ease, Inc., MN, USA). A second-order polynomial model was developed to describe the relationship between the studied variables and the responses. The model's adequacy was assessed by analysis of variance (ANOVA).

Regression coefficients were used to identify the significant terms and factor interactions. Response surface plots curves were generated to visualize effects of the different factors and graphically determine the optimal region. Finally, a software numerical optimization tool was employed to identify the optimal combination of factor levels that maximized the predicted anti-MRSA activity.

### 2.5.3. Artificial Neural Network (ANN) modeling

The MATLAB R2014b Neural Network Fitting Toolbox (Mathworks, Inc., Massachusetts, USA) was used to develop feed forward neural network models. The primary objective of this training was to elucidate the relationship between the input data (independent variables X) and the output data (response Y). This involved fine-tuning of the network parameters to minimize the discrepancy between the model's predicted outputs and the actual target values within the training dataset, thereby ensuring that the prediction model was refined and precise.

Box-Behnken experimental designs (Table 3) from Response surface methodology were utilized to construct the input and output vectors for the neural network model. To ensure consistency and facilitate model training, each variable in the input and output layers was normalized to a range between -1 and 1 by applying the normalization formula given in Eq. (1) ([Salim \*et al.\*, 2019](#)): Where X<sub>min</sub>, X<sub>max</sub> and X<sub>i</sub> are minimum, maximum, and actual data, respectively.

$$\text{Normalized value} = \left[ \frac{2 \times (X_i - X_{\min})}{(X_{\max} - X_{\min})} \right] - 1 \quad (1)$$

**Table 2.** The coded factors in different levels in Box-Behnken design

Factor	Name	Unit	Level		
			-1	0	+1
X <sub>1</sub>	Peptone	g/l	5	10	15
X <sub>2</sub>	CaCO <sub>3</sub>	g/l	1.5	3	4.5
X <sub>3</sub>	pH	–	6	7	8

**Table 3.** Anti-MRSA response Box-Behnken design and artificial neural network (ANN) models of variables (in coded levels)

Block	Runs	Coded values			Experimental anti-MRSA activity (mm)	Predicted anti-MRSA activity RSM (mm)	Predicted anti-MRSA activity ANN (mm)
		X <sub>1</sub> : Peptone	X <sub>2</sub> : CaCO <sub>3</sub>	X <sub>3</sub> : pH			
1	1	-1	0	-1	18	16.59	18.00
1	2	1	0	1	12	12.34	11.50
1	3	1	1	0	13	13.34	13.33
1	4	0	-1	-1	16	16.88	16.00
1	5	0	0	0	14	14.91	15.00
1	6	-1	-1	0	18	17.93	18.50
1	7	0	1	1	15	13.72	15.00
1	8	-1	0	1	10	11.84	12.00
1	9	0	-1	1	12	11.97	12.00
1	10	0	0	0	16	14.91	15.00
1	11	-1	1	0	16	16.84	16.00
1	12	1	0	-1	10	10.43	10.00
1	13	0	0	0	15	14.91	15.00
1	14	0	1	-1	12	11.63	12.00
1	15	1	-1	0	17	15.76	17.00
2	16	0	0	0	16	15.51	15.00
2	17	-1	0	-1	18	17.19	18.00
2	18	0	1	-1	12	12.23	12.00
2	19	0	0	0	16	15.51	15.00
2	20	1	0	1	12	12.94	11.50
2	21	1	-1	0	17	16.36	17.00
2	22	-1	-1	0	19	18.53	18.50
2	23	1	1	0	14	13.94	13.33
2	24	0	-1	-1	16	17.48	16.00
2	25	-1	0	1	14	12.44	12.00
2	26	0	1	1	15	14.32	15.00
2	27	1	0	-1	11	11.03	10.00
2	28	0	0	0	15	15.51	15.00



2	29	-1	1	0	16	17.44	16.00
2	30	0	-1	1	12	12.57	12.00
3	31	-1	0	1	12	11.84	12.00
3	32	0	0	0	14	14.91	15.00
3	33	-1	0	-1	17	16.59	18.00
3	34	-1	1	0	16	16.84	16.00
3	35	0	-1	1	12	11.97	12.00
3	36	0	1	-1	12	11.63	12.00
3	37	0	0	0	14	14.91	15.00
3	38	0	0	0	16	14.91	15.00
3	39	1	1	0	13	13.34	13.33
3	40	0	-1	-1	16	16.88	16.00
3	41	1	0	1	11	12.34	11.50
3	42	1	-1	0	17	15.76	17.00
3	43	-1	-1	0	18	17.93	18.50
3	44	1	0	-1	11	10.43	10.00
3	45	0	1	1	15	13.72	15.00

The final optimized network configuration, achieved through extensive training, conformed to the

mathematical representation outlined in Eq. (2) ([Pathak \*et al.\*, 2015](#)):

$$\text{Inhibition diameter (mm)} = \sum_{j=1}^3 \left\{ \text{purlin} \left[ lw_{j,1} \times \left( \sum_{i=1}^3 \sum_{j=1}^3 \text{tansig} (X_i \times iw_{i,j} + b_j) \right) \right] + a \right\} \quad (2)$$

The connection weights between the hidden and output layers are denoted by  $iw$ , while those from the input to hidden layers are represented by  $iw$ . The bias weights associated with the hidden and output layers are symbolized by  $b_j$  and  $a$ , respectively.

The hidden layer employs the hyperbolic tangent sigmoid transfer function, "*tansig*", for activation, whereas the output layer utilizes the linear transfer function, "*purelin*".

## 2.6. Network architecture and selection of the best topology

To determine the optimal network architecture, a k-fold cross-validation (k=10) was performed by modifying the hidden layer's neuron count from 1 to 15 ([Mechouche \*et al.\*, 2024](#)). Metrics such as mean squared error (MSE) Eq. (3), coefficient of determination ( $R^2$ ) Eq. (4), mean absolute deviation (MAD) Eq. (5), and root mean square error (RMSE) Eq. (6), were used to assess the performance of each network architecture ([Patel \*et al.\*, 2024](#)). The topology exhibiting the best performance according to these criteria was selected as the final architecture for the ANN model.

$$\text{MSE} = \frac{\sum(Y_{\text{exp}} - Y_{\text{pred}})^2}{n} \quad (3)$$

$$R^2 = 1 - \frac{\sum(Y_{\text{exp}} - Y_{\text{pred}})^2}{\sum(Y_{\text{exp}} - \bar{Y}_{\text{exp}})^2} \quad (4)$$

$$\text{MAD} = \sum \left| \frac{Y_{\text{exp}} - Y_{\text{pred}}}{n} \right| \quad (5)$$

$$\text{RMSE} = \sqrt{\frac{\sum(Y_{\text{exp}} - Y_{\text{pred}})^2}{n}} \quad (6)$$

## 2.7. Network generation and sensitivity analysis

Once the optimal architecture was determined, the neural network was generated and trained using the entire experimental dataset. The Levenberg-Marquardt training algorithm was used for network learning. Three sets of the experimental data were randomly selected: training (60 %), testing (20 %), and validation (20 %). The network weights and biases were randomly initialized and iteratively adjusted during the learning phase to minimize the prediction error. To better understand the influence of each input factor ( $X_1$ : Peptone,  $X_2$ :  $\text{CaCO}_3$ ,  $X_3$ : pH) on the response (MRSA inhibition zone diameter), a sensitivity analysis was conducted on the generated ANN model. Two complementary approaches were employed: Garson's algorithm and connection weight approach ([Lau \*et al.\*, 2023](#)).

Garson's algorithm is a commonly used method for determining the relative importance of input factors in a neural network. It is based on the absolute values of the connection weights among the input neurons, hidden neurons, and output neuron ([Garson, 1991](#)). The connection weight approach is an alternative method for evaluating the importance of input factors. Unlike Garson's algorithm, which considers the absolute values of weights, this approach takes into account the sign (positive or negative) of each effect ([Olden \*et al.\*, 2004](#)).

## 2.8. Comparison between RSM and ANN models

Several statistical indicators, including mean absolute percentage error (MAPE), coefficient of determination ( $R^2$ ), adjusted  $R^2$ , root mean squared error (RMSE), average absolute deviation percentage (AAD %), and standard error of prediction percentage (SEP %), were employed to evaluate the predictive abilities of RSM and ANN models Eq. (4-10) ([Vimali \*et al.\*, 2022](#); [Lau \*et al.\*, 2023](#); [Patel \*et al.\*, 2024](#)).

$Y_{\text{exp}}$  represents the values obtained through experimentation, while  $Y_{\text{pred}}$  denotes the corresponding values generated by the predictive model. The total count of data points used as input is symbolized by  $n$ , while  $k$  signifies the count of input variables taken into account. Finally,  $\bar{Y}_{\text{exp}}$  stands for the mean value of the experimental values dataset.

## 2.9. Hybrid ANN-GA optimization

In the present study, a hybrid approach combining an artificial neural network model and a genetic algorithm (GA) was employed to address the modeling and optimization challenges. GA is a well-established optimization tool known for its ability to obtain global solutions rather than local ones ([Kumar \*et al.\*, 2017](#)).



$$\text{Adjusted } R^2 = 1 - \left[ (1 - R^2) - \frac{n - 1}{n - k - 1} \right] \quad (7)$$

$$\text{MAPE} = \sum \left| \frac{Y_{\text{exp}} - Y_{\text{pred}}}{Y_{\text{exp}}} \right| \times \frac{1}{n} \times 100 \quad (8)$$

$$\text{AAD}(\%) = \frac{(\sum |Y_{\text{exp}} - Y_{\text{pred}}|) / \sum Y_{\text{exp}}}{n} \times 100 \quad (9)$$

$$\text{SEP} (\%) = \frac{\text{RMSE}}{\bar{Y}_{\text{exp}}} \times 100 \quad (10)$$

The MATLAB R2014b software (Math Works Inc., USA) with its GA optimization toolbox was used to integrate the ANN-GA approach, aiming to determine the optimal concentrations of culture medium components that maximize the inhibition diameter against MRSA. The well-developed ANN model had served as the fitness function for the GA optimization process. The settings considered for GA tool in this work include the following: size of population: 200; generations: 100; elite number: 2; crossing fraction: 1; direction of migration: forward; stall generation limit: 20; stall time limit: 20, while the other hyper parameters were considered as default ([Alloun \*et al.\*, 2023](#)).

### 2.10. Validation of the RSM-ANN-GA model

To verify the RSM-ANN-GA model, further experiments were conducted using the optimized factor levels. The model's accuracy was evaluated by determining the absolute percentage error (%) between the predicted results and the experimental data. This process was crucial for confirming the model's precision and its predictive capabilities Eq. (11) ([Mechouche \*et al.\*, 2024](#)).

$$\text{Absolute error} (\%) = \frac{|Y_{\text{exp}} - Y_{\text{pred}}|}{Y_{\text{exp}}} \times 100 \quad (11)$$

## 3. Results and Discussion

### 3.1. Phylogenetic analysis

The 16S rRNA gene sequence of strain AR05 was deposited at GenBank under the accession number: MW075678. The phylogenetic analysis of strain AR05 revealed a significant genetic similarity with several species within the *Streptomyces* genus, specifically *S. kurssanovii* NRBC 13192 ([Pridham \*et al.\*, 1958](#)) and *S. ostreogriseus* NBRC 13423 ([Shirling and Gottlieb, 1972](#)), both sharing a sequence similarity of 99.86 %, *S. peucetius* NRBC 100596 (99.58 %) ([Grein \*et al.\*, 1963](#)), and *S. xantholiticus* NRBC (99.57 %) ([Pridham, 1970](#)) (Fig.1). The potential of *Streptomyces* spp. to producing a diverse range of bioactive secondary metabolites, including antibiotics, antifungals, anticancer, and antivirals drugs was widely recognized ([de Lima Procópio \*et al.\*, 2012](#)). Actinobacteria are the main source of around 2/3 of all antibiotics used in clinical practice, with *Streptomyces* being the most prolific genus ([Kemung \*et al.\*, 2018](#)). Many *Streptomyces* spp. have been shown to produce compounds with potent anti-MRSA characteristics. For example, *Streptomyces* sp. MUSC 125 was found to produce a bioactive compound with significant anti-MRSA and anti-biofilm properties ([Kemung \*et al.\*, 2020](#)).

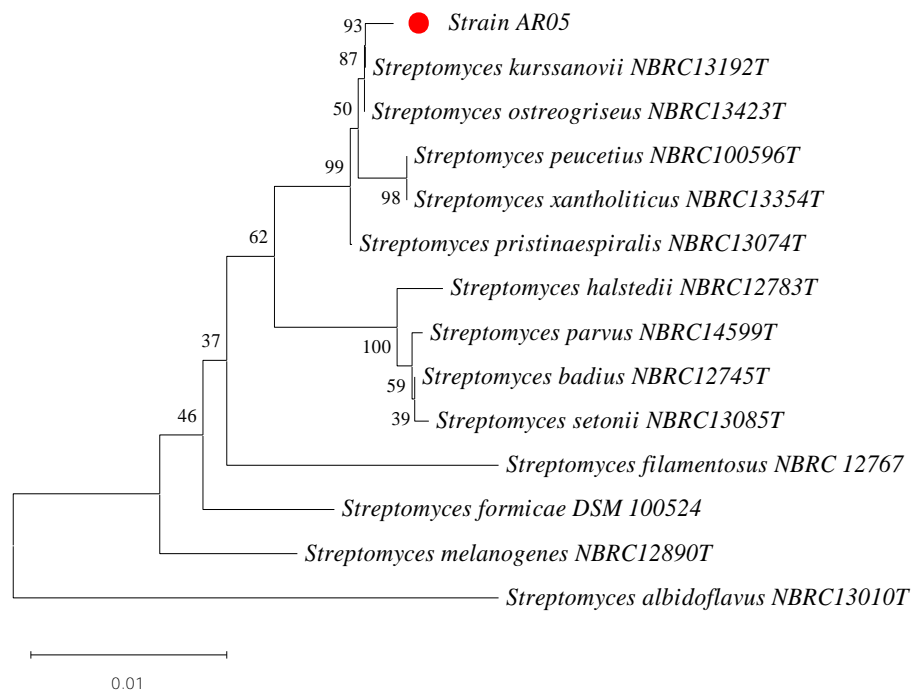


**Fig. 1.** Phylogenetic tree constructed from the 16S rDNA sequence of the *Streptomyces* sp. AR05 strain

Similarly, *Streptomyces* sp. CS392 was shown to produce an antibiotic with strong activity against MRSA (Mander *et al.*, 2013). Other notable examples include *Streptomyces* sp. SD1 (Kalaiyarasi *et al.*, 2020), *Streptomyces* sp. DARP-7 (David *et al.*, 2022), and *Streptomyces* sp. CMSTAAHAL-3 (Selvaraj *et al.*, 2023), all of which have demonstrated promising anti-MRSA potential.

Furthermore, *S. kurssanovii* is known for producing fumaramidmycin; an antibiotic that is effective against both Gram-positive and Gram-negative bacteria, but only when grown on solid media, indicating a strict regulation of secondary metabolite production (Maruyama *et al.*, 1975). This characteristic has inspired us to optimize the production of antimicrobial compounds by AR05 by exploring similar culture conditions.

Regarding *S. ostreogriseus*, this species produces cytotoxic macrolides such as homooligomycin E, which has exhibited anticancer activity against several human tumor cell lines (Kim *et al.*, 1997). The ability of *S. ostreogriseus* to generate bioactive compounds underscores the potential of strain AR05 to produce metabolites with therapeutic properties, which could be exploited to enhance its anti-MRSA activity.

The phylogenetic proximity of strain AR05 to these *Streptomyces* spp. highlights its potential for producing bioactive secondary metabolites. Optimizing the culture medium composition could leverage the conditions that favor metabolite production in related strains, including the use of solid media to stimulate antimicrobial compounds production.

### 3.2. Selection of the best culture medium

The selection of the optimal culture medium for enhancing the anti-MRSA activity of strain AR05 was a critical step in this study. Among the tested media, Glycerol bouillon agar (GBA) demonstrated the highest anti-MRSA activity with an inhibition zone diameter of 15 mm, significantly outperforming the other media such as Yeast malt agar (YMA), which

showed an inhibition diameter of 13.66 mm (Fig. S1). Other media, including Bennett's, czapek and Starch casein agar expressed no activity (Table 4). These results suggest that the nutrient composition of GBA, which includes glycerol and peptone, provides a favorable environment for the production of antimicrobial compounds by AR05 strain.

**Table 4.** Anti-MRSA activity of the AR05 strain as a function of the different culture media

Culture medium	Anti-MRSA activity (Inhibition diameter in mm)
Benett's medium	NA
Czapek medium	NA
Yeast Malt agar	13.66± 0.57
Glycerol Bouillon agar	15.00± 00
Strach Casein agar	NA

Where; NA: no activity, ( $\pm$ ) represents standard error

The GBA medium is crucial for initial screening and studying of antibiotic-producing actinobacteria. According to several previous studies, this medium provides a suitable environment for growth and morphological development of these microorganisms, which is essential for their antibiotic production capabilities ([El Othmany \*et al.\*, 2021](#); [Boukelloul \*et al.\*, 2023](#)). Understanding the conditions under which these microorganisms produce antibiotics can help in discovering new antibiotics and exploring the mechanisms behind their production.

### 3.3. Statistical modeling

#### 3.3.1. Plackett-Burman design

Plackett-Burman (PBD) is a powerful statistical tool for identifying the most significant factors influencing a given response variable such as anti-MRSA activity in a minimal number of experiments. Analysis of variance (ANOVA) of the Plackett-

Burman design results for screening the medium components revealed that peptone:  $X_c$ ,  $CaCO_3$ :  $X_e$ , and pH:  $X_f$  had significant effects ( $p < 0.05$ ) on the anti-MRSA activity of strain AR05 (Table 5). These three factors were thus selected for further optimization *via* response surface methodology. The presence of a significant curvature ( $p < 0.0001$ ) indicated that there is a non-linear relationship between the variables and the response, justifying the use of a second-order experimental design such as the Box-Behnken design to model these interactions ([Latha \*et al.\*, 2017](#)).

The Plackett-Burman design is a valuable tool in the optimization of antibiotic production by *Streptomyces* spp. ([Smaoui \*et al.\*, 2018](#)). The PBD efficiency in experimental design lies in its ability to screen multiple variables simultaneously, thus reducing the number of required experiments compared to full factorial designs ([Patel \*et al.\*, 2024](#)). For instance, a study reported by [Djinni \*et al.\*, \(2018\)](#)

**Table 5.** Analysis of variance results obtained from the Plackett-Burman design

Source	DF	Adj SS	Adj MS	Coef	SE Coef	F-value	p-value
Block	2	1.11	0.5556				
Model	6	73.67	12.28			7.35	< 0.0001
X <sub>a</sub> : Glycerol	1	7.11	7.11	0.4444	0.2154	4.26	0.0511
X <sub>b</sub> : Starch	1	5.44	5.44	0.3889	0.2154	3.26	0.0796
X <sub>c</sub> : Peptone	1	18.78	18.78	-0.7222	0.2154	11.25	0.0019
X <sub>d</sub> : Meat extract	1	7.11	7.11	0.4444	0.2154	4.26	0.0465
X <sub>e</sub> : CaCO <sub>3</sub>	1	13.44	13.44	-0.6111	0.2154	8.05	0.0075
X <sub>f</sub> : pH	1	21.78	21.78	-0.7778	0.2154	13.04	0.0009
Curvature	1	77.36	77.36			46.33	< 0.0001
Residual	35	58.44	1.67				
Total	44	210.58					

Where; DF: Degrees of freedom; Adj SS: Adjusted sum of squares; Adj MS: Adjusted mean square; Coef: Coefficient; SE Coef: Standard error of coefficient

used PBD to optimize the production of the antibiotic Streptazolin by *S. thermoviolaceus* SRC3, and identifying significant factors in just 12 experiments. In another study, [Norouzi et al., \(2019\)](#) employed PBD to identify the significant factors influencing the production of a bioactive compound with anti-MRSA activity from a marine *Streptomyces* strain. The previous analyses have shown that peptone, CaCO<sub>3</sub>, and pH are significant factors, similar to the findings obtained in the present study. Many studies used PBD to screen various medium components for their effect on the production of bioactive metabolites, and highlighted the importance of peptone, starch, and pH in enhancing antibiotic production by *Streptomyces* spp. ([Yi et al., 2015](#)). These examples show that this approach is particularly valuable when resources are limited, as it allows the researchers to quickly identify key variables and focus their subsequent optimization efforts on these factors.

### 3.3.2. Box-Behnken design

To further optimize the significant variables (*i.e.*, peptone: X<sub>1</sub>, CaCO<sub>3</sub>: X<sub>2</sub>, and pH: X<sub>3</sub>) influencing the anti-MRSA activity of *Streptomyces* sp. AR05, Box-

Behnken design was utilized. The experimental design consisted of 15 distinct runs, with each run performed in triplicates (Fig. S2). Results in Table (3) present the coded levels corresponding to the independent variables investigated in this study, as well as the experimental and predicted model responses. The ANOVA analysis results from the Box-Behnken design revealed several key insights into the model's performance and significance (Table 6). With an F-value of 24.34 and a *p*-value of less than 0.0001, the model itself was highly significant and showed a strong fit to the experimental data. The coefficient R<sup>2</sup> is 0.8691, meaning that 86.91 % of the response variability is explained by the model. The adjusted R<sup>2</sup> of 0.8334 supported the model's adequacy and the predicted R<sup>2</sup> of 0.7504 suggested a good predictive power.

In terms of individual factors, X<sub>1</sub>, X<sub>2</sub>, and X<sub>3</sub> were all significant, with *p*-values of less than 0.0001, 0.0002, and 0.0015; respectively, indicating their substantial impact on the response. Significant interaction terms X<sub>1</sub>X<sub>3</sub> and X<sub>2</sub>X<sub>3</sub>, both with *p*-values of less than 0.0001, highlighted the importance of these interactions. The quadratic term for X<sub>3</sub><sup>2</sup> was

**Table 6.** Analysis of variance for experimental results using the Box-Behnken design

Source	DF	Adj SS	Adj MS	Coef	SE Coef	F-value	p-value	VIF
Block	2	3.60	1.80					
Model	9	220.39	24.49			24.34	< 0.0001	
X <sub>1</sub>	1	48.17	48.17	-1.42	0.2048	47.87	< 0.0001	1.0000
X <sub>2</sub>	1	18.38	18.38	-0.8750	0.2048	18.26	0.0002	1.0000
X <sub>3</sub>	1	12.04	12.04	-0.7083	0.2048	11.97	0.0015	1.0000
X <sub>1</sub> X <sub>2</sub>	1	1.33	1.33	-0.3333	0.2896	1.33	0.2580	1.0000
X <sub>1</sub> X <sub>3</sub>	1	33.33	33.33	1.67	0.2896	33.13	< 0.0001	1.0000
X <sub>2</sub> X <sub>3</sub>	1	36.75	36.75	1.75	0.2896	36.52	< 0.0001	1.0000
X <sub>1</sub> <sup>2</sup>	1	0.2585	0.2585	0.1528	0.3014	0.2569	0.6156	1.01
X <sub>2</sub> <sup>2</sup>	1	9.03	9.03	0.9028	0.3014	8.97	0.0052	1.01
X <sub>3</sub> <sup>2</sup>	1	56.77	56.77	-2.26	0.3014	56.42	< 0.0001	1.01
Residual	33	33.21	1.01					
Lack of Fit	27	27.87	1.03			1.16	0.4644	
Pure Error	6	5.33	0.8889					
Total	44	257.20						
Std. Dev.	1.00							
Mean	14.47							
C.V. %	6.93							

Where; X<sub>1</sub>: Peptone. X<sub>2</sub>:CaCO<sub>3</sub>. X<sub>3</sub>: pH; R<sup>2</sup>: 0.8691; Adj R<sup>2</sup>: 0.8334; Pred R<sup>2</sup>: 0.7504; Adeq Precision: 15.6370. DF: Degrees of freedom; Adj SS: Adjusted sum of squares; Adj MS: Adjusted mean square; Coef: Coefficient; SE Coef: Standard error of coefficient; VIF: Variance inflation Factor; C.V. %: Coefficient of variation (%)

notably significant ( $p$ -value < 0.0001), suggesting a strong curvature effect, whereas X<sub>1</sub><sup>2</sup> was not significant ( $p$ -value = 0.6156), indicating negligible curvature for X<sub>1</sub>.

The lack of fit analysis, with an F-value of 1.16 and a  $p$ -value of 0.4644, indicated that the lack of fit was not significant. This suggested that the model adequately captured the data variability and that the residual error was primarily attributed to pure error rather than model inadequacy. The model's adequacy was further confirmed by an Adeq Precision value of 15.6370, which was well above the desirable threshold of 4, indicating a strong signal-to-noise ratio. The coefficient of variation (C.V.) was 6.93 %, reflecting precise model predictions. 3D response surface plots elucidated the complex interactions among the three factors on the inhibition diameter. The X<sub>1</sub>-X<sub>2</sub> plot

revealed a clear trend towards increased inhibition at lower concentrations of peptone and CaCO<sub>3</sub>, indicating a synergistic effect in their reduction Fig. 2(a).

The X<sub>1</sub>-X<sub>3</sub> interaction demonstrated a pronounced curvature; with optimal activity occurring at low peptone levels and moderate pH values Fig. 2(b). The X<sub>2</sub>-X<sub>3</sub> interaction exhibited a saddle-like surface, with maximal inhibition observed at lower levels of both variables, suggesting that reduced CaCO<sub>3</sub> concentrations and slightly acidic conditions enhanced the antimicrobial efficacy Fig. 2(c). These response surfaces revealed the intricate interplay between medium components and environmental conditions, highlighting the need for using a multifactorial strategy to optimize parameters for increased production of antimicrobials.

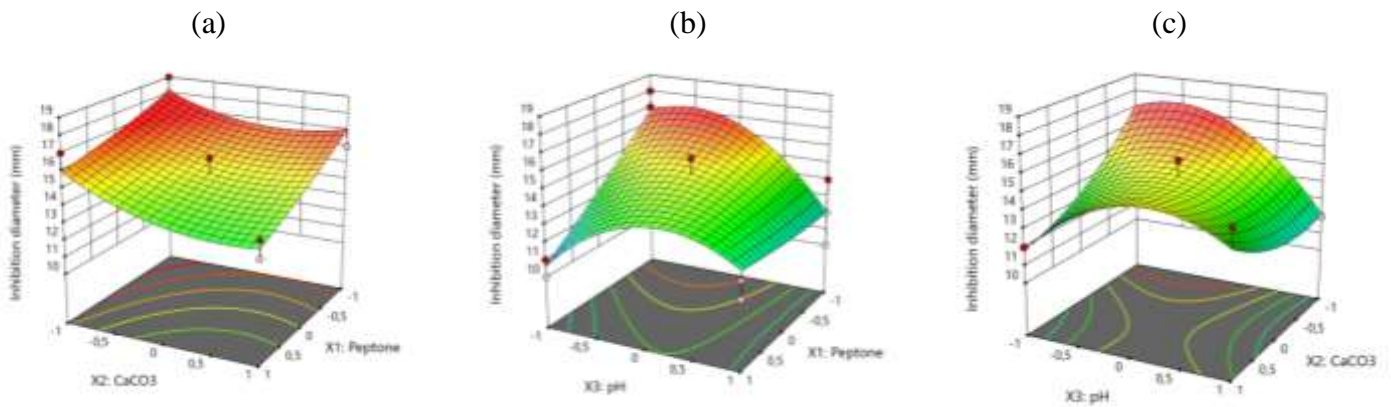


**Fig. 2.** Three-dimensional response surface curve that illustrates how several variables interact to affect anti-SARM activity

The model equation in coded factors (Eq. 12) allowed prediction of the anti-MRSA activity as a function of the levels of the 3 factors. It highlighted the preponderant negative impact of peptone (coefficient -1.42) compared to  $\text{CaCO}_3$  (-0.875) and pH (-0.7083).

$$Y = +15.11 - 1.42 X_1 - 0.8750 X_2 - 0.7083 X_3 - 0.3333 X_1 X_2 + 1.67 X_1 X_3 + 1.75 X_2 X_3 + 0.1528 X_1^2 + 0.9028 X_2^2 - 2.26 X_3^2 \quad (12)$$

The coded factor equation allowed for response predictions at specified factor levels. Typically, factor high levels were assigned a +1 code, while low levels were designated as -1. Comparing the coefficients in the coded equation provided an insight into the relative influence of each factor on the response variable.

Box-Behnken design is a response surface methodology that allowed evaluation of interaction effects between variables and generation of a mathematical model describing the relationship between the factors and the response (Box and Behnken, 1960). The BBD results highlighted the significant effects of peptone,  $\text{CaCO}_3$ , and pH on the anti-MRSA activity of strain AR05. Peptone was

found to have a preponderant negative impact on anti-MRSA activity; with lower concentrations favoring higher inhibition diameters. This observation is consistent with several previous reports that have shown that excessive nitrogen sources can suppress antibiotic production in *Streptomyces* (Asnani *et al.*, 2022).  $\text{CaCO}_3$  and pH also exhibited significant negative effects on anti-MRSA activity; with lower levels and slightly acidic conditions enhancing antimicrobial efficacy. These findings are supported by previous studies that have demonstrated the importance of  $\text{CaCO}_3$  as a buffering agent and pH regulator in *Streptomyces* fermentations (Martinet *et al.*, 2023).

### 3.4. Artificial neural network (ANN) modeling

#### 3.4.1. Architecture and performance

Analysis of ANN performance across various neuron configurations revealed crucial insights for predicting anti-MRSA activity. The optimal architecture was identified with 6 neurons, demonstrating superior performance across all the evaluated metrics.



This configuration minimized MSE to 0.0634 and maximized the coefficient  $R^2$  to 0.7674, thus explaining 76.74 % of the variance in anti-MRSA activity data. Furthermore, it exhibited the lowest MAPE at 65.7076 %, and minimal values for MAD and RMSE. These results indicated that the 6 neuron architecture offered the optimal balance between model complexity and predictive accuracy, thereby providing a reliable foundation for further analysis and optimization of anti-MRSA compound production parameters.

The optimized ANN architecture for predicting anti-MRSA activity consisted of 3 input neurons, 2 hidden layers with 6 neurons each, and 1 output neuron. This structure, coupled with the Levenberg-Marquardt algorithm and sigmoid activation functions, demonstrated robust predictive capabilities (Fig. 3). The model's performance was evidenced by the high correlation coefficients ( $R$ ) for training (0.95707), validation (0.96528), and testing (0.98851) datasets, indicating excellent agreement between predicted and experimental values across all phases of model development.

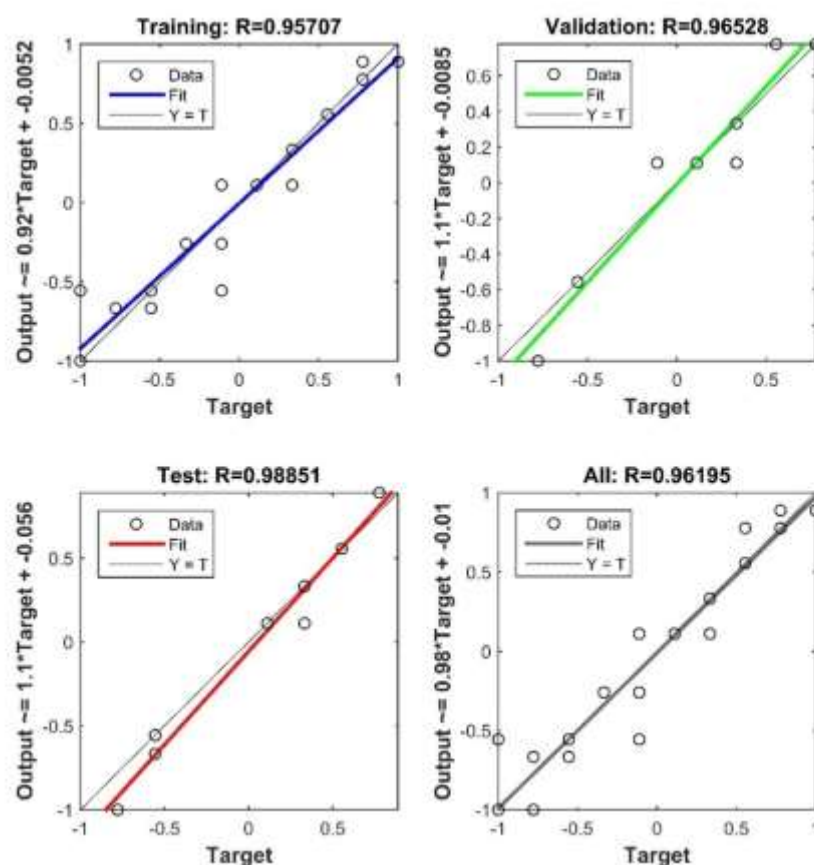


**Fig. 3.** The ANN model's validation, testing, and training

The 3D response surface plots generated by ANN model revealed complex interactions between the input variables. The  $X_1$ - $X_2$  interaction (Peptone vs.  $\text{CaCO}_3$ ) exhibited a saddle-like surface, with maximum inhibition observed at low peptone and moderate  $\text{CaCO}_3$  levels Fig. 4(a). The  $X_1$ - $X_3$  interaction (Peptone vs. pH) revealed a highly non-linear relationship. The maximum inhibition diameter occurred at low peptone concentrations across a range of pH values, with a notable peak in the response surface Fig. 4(b). The  $X_2$ - $X_3$  interaction ( $\text{CaCO}_3$  vs. pH) showed a pronounced peak at moderate  $\text{CaCO}_3$  levels and slightly acidic pH Fig. 4(c).

This highlighted the importance of precise pH control in conjunction with appropriate  $\text{CaCO}_3$  concentration for maximizing antimicrobial efficacy. The complex surface topology indicated that small variations in these parameters can significantly impact the inhibition diameter. In terms of comparison, the response surfaces generated by ANN exhibited significantly more complex and nonlinear topologies than those typically obtained by RSM. This suggested that ANN captures more subtle and complex interactions between the variables that the RSM might not detect.

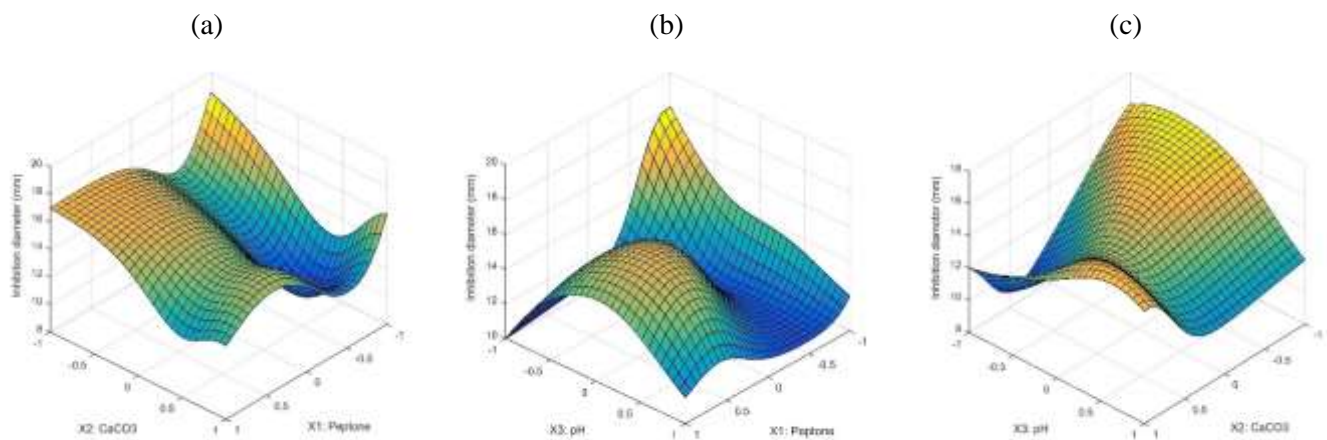


**Fig. 4:** Three-dimensional ANN model surface curve that illustrates how several variables interact to affect anti-SARM activity

The artificial neural networks are a potent substitute for response surface methodology in the modeling and optimization of intricate bioprocesses such as *Streptomyces*' synthesis of antibiotics. ANNs may learn from examples to approximate complex non-linear relationships between input variables and output responses. They are inspired by the structure and operation of biological neural networks (Ekenyong *et al.*, 2021). In contrast to RSM, which

relies on predefined polynomial models, ANNs can adapt to the inherent complexity of biological systems without prior assumptions about the underlying relationships (Lee *et al.*, 2022). This flexibility allowed ANNs to capture subtle interactions and non-linearity that may be overlooked by RSM, leading to more accurate predictions and optimization results (Rayavarapu *et al.*, 2019).

### 3.4.2. Artificial neural network sensitivity analysis

Important information about the relative significance of input variables in modifying anti-MRSA activity was obtained from the sensitivity analysis, which was carried out using both Garson's Algorithm and the Connection Weight approach. (Table 7). Garson's Algorithm revealed that peptone concentration had the most substantial impact (36.51 %) on anti-MRSA activity, closely followed by CaCO<sub>3</sub> (35.94 %); with pH having a comparatively lower (27.53 %) but still significant, influence. The

Connection Weight approach considered the direction and strength of effects. While peptone concentration remained the most influential factor (-3.91), its large negative value suggested that increasing peptone concentration generally led to a decrease in anti-SARM activity. The pH emerged as the second most important factor in this analysis (-1.5933), also with a negative effect, indicating that lower pH values tend to enhance anti-SARM activity. CaCO<sub>3</sub>, while still important, showed a less pronounced negative effect (-0.99).

**Table 7.** Sensitivity analysis

	Garson's method		Connection Weight method	
	Relative importance (%)	Inputs ranked according to relative relevance	Connection weight approach (S <sub>i</sub> values)	Inputs ranked according to relative relevance
X <sub>1</sub> : Peptone	36.5189	1	-3.9145	1
X <sub>2</sub> : CaCO <sub>3</sub>	35.9465	2	-0.9893	3
X <sub>3</sub> : pH	27.5346	3	-1.5933	2

The discrepancy in the ranking of pH and CaCO<sub>3</sub> between the connection weight method and Garson's algorithm can be attributed to the inherent differences in how these methods assessed variable importance. Garson's approach considers the absolute values of the connection weights as a measure of the overall influence of each input variable on the output, regardless of direction of the effect (Lau *et al.*, 2023).

As opposed to this, the connection weight technique considers the weights' sign (positive or negative), providing information on the direction and strength of each variable's influence on the response (Lau *et al.*, 2023). Furthermore, the complex, non-linear relationships between the input variables and

the anti-MRSA activity, as evidenced from the response surface plots, may contribute to the observed differences in ranking. The CaCO<sub>3</sub> vs. pH plot, for instance, revealed a pronounced peak at moderate CaCO<sub>3</sub> levels and slightly acidic pH, indicating a strong interaction effect. This suggested that while CaCO<sub>3</sub> may have a broader overall impact on the response (as captured by Garson's algorithm); the directionality of its effect was highly dependent on the pH level, which was better reflected by the connection weight approach. Reconciling of these differences requires a holistic interpretation of the sensitivity analysis results in conjunction with the insights gained from the response surface analysis.

### 3.5. RSM-ANN comparison

The performance metrics calculated for RSM and ANN models demonstrated that in forecasting the inhibition activity, the ANN model performed better than the RSM model. The ANN model exhibited a RMSE of 0.6694; substantially lower than that of the RSM model (0.8581). This difference indicated that the predictions of ANN model were in line with the experimental values more than those of the RSM model. Furthermore, the ANN model demonstrated a MAPE of 3.0157%, in contrast to 4.9649 % for the RSM model. This metric quantified the average error in terms of percentage, providing an indication of the prediction accuracy. The lower MAPE of ANN model suggested that its predictions were more accurate than those of the RSM model.

To further assess the goodness of fit of the models, the coefficient  $R^2$  was calculated. The ANN model had an  $R^2$  of 0.9216, implying that it explained 92.16 % of the variability in the response variable. In comparison, the RSM model had an  $R^2$  of 0.8712. The adjusted  $R^2$ , which considered the number of predictor variables in the model, was also higher for the ANN model (0.9159) than for the RSM model (0.8617). These findings implied that the ANN model fitted the data more accurately and at a greater ability to explain the variability in the response, corroborating the findings from the RMSE and MAPE metrics.

To assess the accuracy and dependability of the model's predictions, the SEP % and the AAD % were calculated. The SEP expressed the prediction error as a percentage of the mean response variable. The ANN model had an SEP of 4.6275 %, while the RSM model had an SEP of 5.9319 %. Lower SEP of the ANN model indicated that its predictions were more accurate and reliable compared to those of the RSM model. Similarly, the AAD measured the mean absolute difference between the experimental and predicted values, expressed as a percentage of the mean experimental values. The ANN model had an AAD of 2.8157 %, compared to 4.9155 % for the RSM model.

The obtained metrics confirmed that the ANN model provided more accurate predictions than the RSM model; this finding is in line with numerous previous studies that have reported the advantages of ANNs over RSM for bioprocess modeling and optimization ([Vimali \*et al.\*, 2022](#); [Patel \*et al.\*, 2024](#)). The ability of ANNs to approximate complex non-linear relationships without prior assumptions about the model form enabled them to capture the inherent complexity of biological systems more effectively than RSM. Moreover, the hybridization of ANNs with GA for global optimization allowed for identification of optimal conditions that may be overlooked by the classical gradient-based methods used in RSM ([Kumar \*et al.\*, 2017](#)).

### 3.6. ANN-GA analysis

The hybridization of artificial neural networks with genetic algorithms has emerged as a powerful approach for optimizing complex bioprocesses, including antibiotic production by *Streptomyces* spp. ([Kumar \*et al.\*, 2017](#)). In this study, the ANN-GA hybrid approach allowed for determination of optimal concentrations of peptone (5.34 g/l),  $\text{CaCO}_3$  (1.54 g/l), and pH (6.07), which maximized the predicted anti-MRSA activity (21.65 mm) of strain AR05 (Table 8).

The significant improvement in anti-MRSA activity achieved through the ANN-GA optimization process can be attributed to several factors. First, the ability of ANN to capture the intricate and non-linear connections among the input variables (peptone,  $\text{CaCO}_3$ , and pH), and the output response (anti-MRSA activity) that allowed for a more accurate representation of the underlying biological processes ([Rayavarapu \*et al.\*, 2019](#)). It is possible to identify the ideal conditions with this improved understanding of the system dynamics, which may not be evident using conventional statistical techniques. Second, the GA's global optimization capabilities ensures that the search for optimal conditions is not limited to local optima, which is a common limitation of the gradient-based optimization methods used in RSM ([Kumar \*et al.\*, 2017](#)).

**Table 8.** Optimal culture conditions for maximizing anti-MRSA activity

Input variables	Before optimization	RSM model	ANN-GA model
Peptone (g/l)	10	5.04 (-0.991)	5.34 (-0.931)
CaCO <sub>3</sub> (g/l)	3	1.53 (-0.975)	1.54 (-0.969)
pH	7	6.13 (-0.870)	6.07 (-0.928)
Predicted anti-SARM activity (mm)	–	19.87	21.65
Experimental anti-SARM activity (mm)*	15.00± 0	18.33± 0.57	22.33± 0.57

Where; \* The anti-SARM potency was evaluated at the 5-d point during the fermentation process. The reported values represent the average of three independent measurements, with the corresponding standard deviation ( $\pm$ SD) provided

By exploring a wider range of possible solutions, the ANN-GA approach increases the likelihood of identifying the most favorable combination of factor levels for maximizing antimicrobial production. Finally, the ANN-GA optimization process progressively refines the model in a step-by-step manner, allowing for identification of increasingly optimal conditions. As GA generates new candidate solutions based on ANN's predictions, the model is continuously updated with new experimental data, leading to a more accurate representation of the system, and consequently more effective optimization ([Alloun \*et al.\*, 2023](#)).

### 3.7. RSM-ANN-GA model validation

The ANN-GA optimized conditions for maximizing anti-MRSA activity in strain AR05 demonstrated significant improvements over both the initial and RSM-optimized conditions. The initial culture conditions (10 g/l peptone, 3 g/l CaCO<sub>3</sub>, pH 7) resulted in an experimental anti-MRSA activity of 15.00 mm. In comparison, the RSM-optimized conditions (5.04 g/l peptone, 1.53 g/l CaCO<sub>3</sub>, pH 6.13) predicted an anti-MRSA activity of 19.87 mm, which was experimentally validated to be 18.33 mm. The ANN-GA approach further refined these conditions, suggesting optimal concentrations of 5.34 g/l peptone, 1.54 g/l CaCO<sub>3</sub>, and a pH of 6.07. These optimized conditions predicted an anti-MRSA activity

of 21.65 mm, which was experimentally confirmed to be 22.33 mm, representing a 48.87 % increase from the initial conditions and a 21.82 % improvement over the RSM-optimized conditions.

Moreover, experimental validation of ANN-GA hybrid model under the optimized conditions yielded an anti-MRSA activity very close to the predicted value (22.33 mm vs. 21.65 mm), representing an absolute error of only 3.14 %. This excellent agreement between predicted and experimental results confirmed the validity and robustness of the developed model. Prediction errors below 5 % are considered highly satisfactory for bioprocesses, given their inherent variability ([Nalini \*et al.\*, 2021](#); [Lau \*et al.\*, 2023](#)). The low absolute error observed in this study further validated the ANN-GA approach as a reliable tool for optimizing culture conditions to enhance antimicrobial production by *Streptomyces* spp. The successful validation of ANN-GA hybrid model in this study is consistent with the findings of similar studies in the literatures that have employed this approach for optimizing bioprocesses and enhancing secondary metabolite production. For example, [Salim \*et al.\*, \(2019\)](#) used an ANN-GA approach to optimize the production of L-methioninase; an enzyme with potential applications in cancer treatment, from *Trichoderma harzianum*. The optimized conditions predicted by the model resulted in a 2.6-fold increase in L-methioninase



activity compared to the initial conditions, with a low absolute error of 3.8 % between the predicted and experimental values ([Salim \*et al.\*, 2019](#)). Similarly, [Joshi and Singhal, \(2016\)](#) applied an ANN-GA hybrid approach to optimize the production of zeaxanthin; a valuable carotenoid pigment, by *Paracoccus zeaxanthinifaciens*. The optimized conditions led to a 1.5-fold increase in zeaxanthin production, with a high correlation coefficient ( $R^2 = 0.9989$ ) between the predicted and experimental values. In the context of antimicrobial production by *Streptomyces* spp., [Norouzi \*et al.\*, \(2019\)](#) study employed response surface methodology to optimize the production of a bioactive compound with anti-MRSA activity from a marine *Streptomyces* strain. The optimized conditions resulted in a 2.4-fold increase in antimicrobial activity compared to the initial conditions, with a low absolute error of 4.2 % between the predicted and experimental values. The validation outcomes of this study, with a 48.87 % increase in anti-MRSA activity and a low absolute error of 3.14 %, are comparable to or better than those reported in similar studies.

However, it is essential to acknowledge the potential limitations of the model. First, the quantity and quality of the experimental data used for training and validation may have an impact on the model's performance. Ensuring that the data covers a wide range of conditions and is representative of the system's behavior is crucial for developing a reliable and generalizable model ([Vimali \*et al.\*, 2022](#)). Second, the model's predictive capabilities may be limited to the specific strain and range of culture conditions investigated in this study. Extrapolating the model's predictions beyond the studied design space or applying them to other *Streptomyces* strains may require further validation and model refinement ([Beg, 2021](#)). Finally, the ANN-GA approach, like any modeling technique, is a simplification of the complex biological processes underlying antimicrobial production. While the model has demonstrated excellent predictive performance, it may not capture all the intricate interactions and regulatory

mechanisms involved in secondary metabolites biosynthesis ([Djinni \*et al.\*, 2018](#)).

Despite these potential limitations, the ANN-GA hybrid model developed in this study has proven to be a reliable and effective tool for optimizing culture conditions to enhance anti-MRSA activity in strain AR05. The model's robustness and predictive accuracy highlighted the potential of this approach for accelerating the discovery and development of novel antimicrobial compounds from *Streptomyces* spp.

## Conclusion

In this study, we successfully optimized the production of anti-MRSA compounds by *Streptomyces* sp. AR05 using an integrated RSM-ANN-GA approach. The strain isolated from hydrocarbon-contaminated soil has shown promise as a source for novel antibacterial compounds. Application of statistical modeling, machine learning, and global optimization techniques allowed for a comprehensive understanding of the complex relationships between culture conditions and antimicrobial activity. ANN model proved superior to RSM in capturing the non-linear interactions between the key factors influencing anti-MRSA activity; namely peptone,  $\text{CaCO}_3$ , and pH. Sensitivity analysis revealed the relative importance of these factors, with peptone having the most substantial impact on antimicrobial production. Hybridization of ANN model with GA enabled the identification of optimal culture conditions, leading to a significant improvement in anti-MRSA activity compared to the initial and RSM-optimized conditions. Successful validation of the optimized conditions; with a low absolute error between the predicted and experimental values, confirmed the robustness and reliability of the developed RSM-ANN-GA model. This integrated approach offers a powerful tool for optimizing bioprocesses and improving *Streptomyces* strains capacity to produce useful secondary metabolites. The optimized production of antimicrobial compounds by *Streptomyces* sp. AR05 highlights the untapped potential of actinobacteria obtained from



underexplored and extreme environments as a rich source of bioactive metabolites.

### Acknowledgement

None.

### Conflict of interests

The authors have no relevant financial conflicts of interest to disclose.

### Funding source

This work was supported by the Directorate-General for Scientific Research and Technological Development (DGRSDT), Algeria (Fund code no.: E2710204).

### Ethical approval

Non-applicable.

### Author's Contributions

F.M.: Conceptualization, Methodology, Formal analysis, Software, Writing - Original Draft, Supervision; A.K.: Conceptualization, Methodology, Formal analysis, Writing - Review & Editing; R.M.: Conceptualization, Methodology, Formal analysis, Writing - Review & Editing; M.S.M.: Conceptualization, Methodology, Writing - Review & Editing; C.E.H.M.: Conceptualization, Methodology, Writing - Review & Editing; A.B.: Writing - Review & Editing.

### 4. References

**Aburas, M. (2022).** Characterization and Identification of *Pantoea calida* from Contaminated Soil and Its Biocontrol by *Streptomyces coeruleorubidus*. *World Journal of Environmental Biosciences*. 11(3): 50-56. <https://doi.org/10.51847/JXVBFWSN1>.

**Alloun, W.; Berkani, M.; Benaissa, A.; Shavandi, A.; Gares, M.; Danesh, C. et al. (2023).** Waste valorization as low-cost media engineering for auxin

production from the newly isolated *Streptomyces rubrogriseus* AW22: Model development. *Chemosphere*. 326: 138394. <https://doi.org/10.1016/J.CHEMOSPHERE.2023.138394>.

**Antoraz, S.; Santamaría, R.I.; Díaz, M.; Sanz, D. and Rodríguez, H. (2015).** Toward a new focus in antibiotic and drug discovery from the *Streptomyces* arsenal. *Frontiers in Microbiology*. 6: 135327. <https://doi.org/10.3389/FMICB.2015.00461>.

**Asnani, A.; Purwanti, A.; Bakrudin, W.A. and Anjarwati, D.U. (2022).** The Production of *Streptomyces* W-5B Extract for Antibiofilm against Methicillin-resistant *Staphylococcus aureus*. *Journal of Pure and Applied Microbiology*. 16(1): 337–346. <https://doi.org/10.22207/JPAM.16.1.23>.

**Atlas, R.M. (2010).** Handbook of Microbiological Media (4<sup>th</sup> Edition). CRC Press. pp. 1935. <https://doi.org/10.1201/EBK1439804063>.

**Beg, S. (2021).** Design of Experiments for Pharmaceutical Product Development: Volume II: Applications and Practical Case studies. 2: 1-188. <https://doi.org/10.1007/978-981-33-4351-1>.

**Bhakyashree, K. and Kannabiran, K. (2020).** Actinomycetes mediated targeting of drug resistant MRSA pathogens. *Journal of King Saud University-Science*. 32(1): 260-264. <https://doi.org/10.1016/J.JKSUS.2018.04.034>.

**Boukelloul, I.; Aouar, L.; Chekara Bouziani, M.; Zellagui, A.; Derdour, M. et al. (2023).** Antagonism and plant growth promoting traits of actinomycetes isolated from the rhizosphere of halophyte *Atriplex halimus* L. *Notulae Scientia Biologicae*. 15(1): 11437-11437. <https://doi.org/10.55779/NSB15111437>.

**Box, G.E.P. and Behnken, D.W. (1960).** Some New Three Level Designs for the Study of Quantitative Variables. *Technometrics*. 2(4): 455-475. <https://doi.org/10.1080/00401706.1960.10489912>.

- CLSI. (2023). Performance Standards for Antimicrobial Susceptibility Testing (33<sup>rd</sup> Edition. Vol. M100). Clinical and Laboratory Standards Institute.
- Dar, M.S. and Ahmad, I. (2024).** Screening and evaluation of antibacterial active strains of Actinomycetes isolated from Northern Indian soil for biofilm inhibition against selected ESKAPE pathogens. *Journal of Umm Al-Qura University for Applied Sciences*. 1-16. <https://doi.org/10.1007/s43994-024-00164-8>
- David, M.L.R.; Innasimuthu, G.M.; Rajaram, S.K. and Nooruddin, T. (2022).** An endophytic *Streptomyces* sp. DARP-7 isolated from coastal lichen and enhancement of its antibacterial metabolite production using response surface methodology. *South African Journal of Botany*. 151: 636-648. <https://doi.org/10.1016/J.SAJB.2022.10.022>.
- de Lima Procópio, R.E.; da Silva, I.R.; Martins, M.K.; de Azevedo, J.L. and de Araújo, J.M. (2012).** Antibiotics produced by *Streptomyces*. *The Brazilian Journal of Infectious Diseases: An Official Publication of the Brazilian Society of Infectious Diseases*. 16(5): 466-471. <https://doi.org/10.1016/J.BJID.2012.08.014>.
- Djinni, I.; Djoudi, W.; Souagui, S.; Rabia, F.; Rahmouni, S.; Mancini, I. et al. (2018).** *Streptomyces thermoviolaceus* SRC3 strain as a novel source of the antibiotic adjuvant streptazolin: A statistical approach toward the optimized production. *Journal of Microbiological Methods*. 148: 161-168. <https://doi.org/10.1016/J.MIMET.2018.04.008>.
- Ekpenyong, M.; Asitok, A.; Antai, S.; Ekpo, B.; Antigha, R. and Ogarekpe, N. (2021).** Statistical and Artificial Neural Network Approaches to Modeling and Optimization of Fermentation Conditions for Production of a Surface/Bioactive Glyco-lipo-peptide. *International Journal of Peptide Research and Therapeutics*. 27(1): 475-495. <https://doi.org/10.1007/S10989-020-10094-8>.
- El Othmany, R.; Zahir, H.; Zanane, C.; El Louali, M. and Latrache, H. (2021).** Influence of consistency and composition of growth medium on surface physicochemical properties of *Streptomyces*. *Journal of Pure and Applied Microbiology*. 15(3): 1705-1715. <https://doi.org/10.22207/JPAM.15.3.67>.
- Evangelista-Martínez, Z.; Ríos-Muñiz, D.E.; Gómez-Cano, J.; Montoya-Hidalgo, A.C.; Ochoa-Solórzano, R.E.; Evangelista-Martínez, Z. et al. (2022).** Antibacterial activity of *Streptomyces* sp. Y15 against pathogenic bacteria and evaluation of culture media for antibiotic production. *TIP. Revista Especializada En Ciencias Químico-Biológicas*. 25: 1-12. <https://doi.org/10.22201/FESZ.23958723E.2022.415>.
- Garson, D.G. (1991).** Interpreting neural-network connection weights. *AI Expert*. 6: 47-51.
- Goodfellow, M.; O'Donnell, A.G.; Baumberg, S.; Hunter, I. and Rhodes, P.M. (1989).** *Microbial Products: New Approaches*. Baumberg, S.; Hunter, I. and Rhods, M (Editors). Cambridge University Press. Cambridge. pp. 343-383.
- Grein, A.; Spalla, C.; Di Marco, A. and Canevazzi, G. (1963).** Descrizione e classificazione di un attinomicete (*Streptomyces peucetius* sp. nova) produttore di una sostanza ad attività antitumorale-La Daunomicina. *Giornale Di Microbiologia*. 11:109-118.
- Hopwood, D.A. (1985).** *Genetic manipulation of Streptomyces: a laboratory manual*. John Innes Foundation. Norwich, UK and Cold Spring Harbour Laboratory. 356. [https://doi.org/10.1016/0307-4412\(86\)90228-1](https://doi.org/10.1016/0307-4412(86)90228-1).
- Jalal, B.K. and Hasan, A.H. (2021).** Molecular and Phenotypic Characterization of Novel *Streptomyces* Species Isolated from Kurdistan Soil and its Antibacterial Activity Against Human Pathogens. *Jordan Journal of Biological Sciences*. 14(3): 441-451. <https://doi.org/10.54319/JJBS/140309>.

- Joshi, C. and Singhal, R.S. (2016).** Modelling and optimization of zeaxanthin production by *Paracoccus zeaxanthinifaciens* ATCC 21588 using hybrid genetic algorithm techniques. *Biocatalysis and Agricultural Biotechnology*. 8: 228-235. <https://doi.org/10.1016/J.BCAB.2016.10.004>.
- Kalaiyarasi, M.; Ahmad, P. and Vijayaraghavan, P. (2020).** Enhanced production antibiotics using green gram husk medium by *Streptomyces* sp. SD1 using response surface methodology. *Journal of King Saud University-Science*. 32(3): 2134-2141. <https://doi.org/10.1016/J.JKSUS.2020.02.014>.
- Kemung, H.M.; Tan, L.T.H.; Chan, K.G.; Ser, H.L.; Law, J.W.F.; Lee, L.H. et al. (2020).** *Streptomyces* sp. Strain MUSC 125 from Mangrove Soil in Malaysia with Anti-MRSA, Anti-Biofilm and Antioxidant Activities. *Molecules*. 25(15): 3545. <https://doi.org/10.3390/MOLECULES25153545>.
- Kemung, H.M.; Tan, L.T.H.; Khan, T.M.; Chan, K.G.; Pusparajah, P.; Goh, B.H. et al. (2018).** *Streptomyces* as a prominent resource of future anti-MRSA drugs. *Frontiers in Microbiology*. 9: 377137. <https://doi.org/10.3389/FMICB.2018.02221>.
- Kim, H.S.; Bang, H.J.; Lee, S.Y.; Yoo, O.J.; Yoo, J.C.; Kim, Y.H. et al. (1997).** 44-Homooligomycin E, a New Cytotoxic Macrolide Antibiotic from *Streptomyces ostreogriseus*. *Bioscience, Biotechnology, and Biochemistry*. 61(2): 378-380. <https://doi.org/10.1271/BBB.61.378>.
- Kumar, V.; Chhabra, D. and Shukla, P. (2017).** Xylanase production from *Thermomyces lanuginosus* VAPS-24 using low cost agro-industrial residues via hybrid optimization tools and its potential use for saccharification. *Bioresource Technology*. 243: 1009-1019. <https://doi.org/10.1016/J.BIORTECH.2017.07.094>.
- Latha, S.; Sivaranjani, G. and Dhanasekaran, D. (2017).** Response surface methodology: A non-conventional statistical tool to maximize the throughput of *Streptomyces* species biomass and their bioactive metabolites. *Critical Reviews in Microbiology*. 43(5): 567-582. <https://doi.org/10.1080/1040841X.2016.1271308>.
- Lau, H.L.; Wong, F.W.F.; Rahman, R.N.Z.R.A.; Mohamed, M.S.; Ariff, A.B. and Hii, S.L. (2023).** Optimization of fermentation medium components by response surface methodology (RSM) and artificial neural network hybrid with genetic algorithm (ANN-GA) for lipase production by *Burkholderia cenocepacia* ST8 using used automotive engine oil as substrate. *Biocatalysis and Agricultural Biotechnology*. 50: 102696. <https://doi.org/10.1016/J.BCAB.2023.102696>.
- Lee, M.H.; Lu, W.B.; Lu, M.K. and Chang, F.J. (2022).** A hybrid of response surface methodology and artificial neural network in optimization of culture conditions of mycelia growth of *Antrodia cinnamomea*. *Biomass and Bioenergy*. 158: 106349. <https://doi.org/10.1016/J.BIOMBIOE.2022.106349>.
- Lertcanawanichakul, M. and Chawawisit, K. (2019).** Identification of *Streptomyces* spp. isolated from air samples and its cytotoxicity of anti-MRSA bioactive compounds. *Biocatalysis and Agricultural Biotechnology*. 20: 101236. <https://doi.org/10.1016/J.BCAB.2019.101236>.
- Mander, P.; Choi, Y.H.; Seong, J.H.; Na, B.H.; Cho, S.S.; Lee, H.J. et al. (2013).** Statistical optimization of a multivariate fermentation process for enhancing antibiotic activity of *Streptomyces* sp. CS392. *Archives of Pharmacal Research*. 36(8): 973-980. <https://doi.org/10.1007/S12272-013-0140-4>.
- Martinet, L.; Naômé, A.; Rezende, L.C.D.; Tellatin, D.; Pignon, B.; Docquier, J.D. et al. (2023).** Lunaemycins, new cyclic hexapeptide antibiotics from the cave moonmilk-dweller *Streptomyces lunaelactis* MM109T. *International Journal of Molecular Sciences*. 24(2): 1114. <https://doi.org/10.3390/IJMS24021114/S1>.
- Maruyama, H.B.; Suhara, Y.; Suzuki-Watanabe, J.; Maeshima, Y.; Shimizu, N.; Ogura-Hamada, M.**

**et al. (1975).** A new antibiotic, fumaramidmycin i. Production, biological properties and characterization of producer strain. *The Journal of Antibiotics*. 28(9): 636-647.

<https://doi.org/10.7164/ANTIBIOTICS.28.636>.

**Mechouche, M.S.; Merouane, F.; Addad, A.; Karmazin, L.; Boukherroub, R. and Lakhdari, N. (2024).** Enhanced biosynthesis of coated silver nanoparticles using isolated bacteria from heavy metal soils and their photothermal-based antibacterial activity: integrating Response Surface Methodology (RSM) Hybrid Artificial Neural Network (ANN)-Genetic Algorithm (GA) strategies. *World Journal of Microbiology and Biotechnology*. 40(8): 1-20.  
<https://doi.org/10.1007/S11274-024-04048-1>.

**Mechouche, M.S.; Merouane, F.; Messaad, C.E.H.; Golzadeh, N.; Vasseghian, Y. and Berkani, M. (2022).** Biosynthesis, characterization, and evaluation of antibacterial and photocatalytic methylene blue dye degradation activities of silver nanoparticles from *Streptomyces tuiurus* strain. *Environmental Research*. 204: 112360.  
<https://doi.org/10.1016/J.ENVRES.2021.112360>.

**Nalini, S.; Inbakandan, D.; Stalin Dhas, T. and Sathiyamurthi, S. (2021).** Optimization of biosurfactant production by marine *Streptomyces yousoufiensis* SNSAA03: A comparative study of RSM and ANN approach. *Results in Chemistry*. 3: 100223.  
<https://doi.org/10.1016/J.RECHEM.2021.100223>.

**Norouzi, H.; Khorasgani, M.R. and Danesh, A. (2019).** Anti-MRSA activity of a bioactive compound produced by a marine *Streptomyces* and its optimization using statistical experimental design. *Iranian Journal of Basic Medical Sciences*. 22(9): 1073-1084.  
<https://doi.org/10.22038/IJBMS.2019.33880.8058>.

**Olden, J.D.; Joy, M.K. and Death, R.G. (2004).** An accurate comparison of methods for quantifying variable importance in artificial neural networks using simulated data. *Ecological Modelling*. 178(3-4): 389-

397.

<https://doi.org/10.1016/J.ECOLMODEL.2004.03.013>.

**Patel, A.; Patel, P.; Parmar, M. and Gosai, H. (2024).** Employing RSM and ANN-based applications for modelling enhanced bacterial cellulose production from pineapple peel waste using *Komagateibacter saccharivorans* APPK1. *Chemical Engineering Journal*. 480: 148057.  
<https://doi.org/10.1016/J.CEJ.2023.148057>.

**Pathak, L.; Singh, V.; Niwas, R.; Osama, K.; Khan, S.; Haque, S. et al. (2015).** Artificial Intelligence versus Statistical Modeling and Optimization of Cholesterol Oxidase Production by using *Streptomyces* Sp. *PLOS ONE*. 10(9): e0137268.  
<https://doi.org/10.1371/JOURNAL.PONE.0137268>.

**Plackett, R.L. and Burman, J.P. (1946).** The design of optimum multifactorial experiments. *Biometrika*. 33(4): 305-325.  
<https://doi.org/10.1093/BIOMET/33.4.305>.

**Pridham, T. (1970).** New names and new combinations in the order Actinomycetales Buchanan 1917. *Bulletin of the United States Department of Agriculture*. 1424: 1-55.

**Pridham, T.G.; Hesseltine, C.W. and Benedict, R.G. (1958).** A Guide for the Classification of Streptomyces According to Selected Groups. Placement of Strains in Morphological Sections. *Applied Microbiology*. 6(1): 52-79.  
<https://doi.org/10.1128/AM.6.1.52-79.1958>.

**Rachid, S. (2012).** Mutation of RNA Polymerase-subunit confers in both enhancement of environmental bioremediation and antibiotic production in a *Streptomyces* species. *WIT Transactions on Engineering Sciences*. 80: 279-291.  
<https://doi.org/10.2495/PMR120251>.

**Rayavarapu, B.; Tallapragada, P. and Usha, M.S. (2019).** Statistical optimization of  $\gamma$ -aminobutyric acid production by response surface methodology and artificial neural network models using *Lactobacillus*



*fermentum* isolated from palm wine. *Biocatalysis and Agricultural Biotechnology*. 22: 101362. <https://doi.org/10.1016/J.BCAB.2019.101362>.

**Salim, N.; Santhiagu, A. and Joji, K. (2019).** Process modeling and optimization of high yielding L-methioninase from a newly isolated *Trichoderma harzianum* using response surface methodology and artificial neural network coupled genetic algorithm. *Biocatalysis and Agricultural Biotechnology*. 17: 299-308. <https://doi.org/10.1016/J.BCAB.2018.11.032>.

**Selvaraj, J.N.; Ganapathi, U.; Vincent, S.G.P.; Ramamoorthy, S. and Thavasimuthu, C. (2023).** Statistical optimization of media components for antibiotic production in *Streptomyces* sp. CMSTAAHAL-3. *Electronic Journal of Biotechnology*. 65: 1-13. <https://doi.org/10.1016/J.EJBT.2023.03.005>.

**Sharma, M. and Manhas, R.K. (2019).** Purification and characterization of actinomycins from *Streptomyces* strain M7 active against methicillin resistant *Staphylococcus aureus* and vancomycin resistant *Enterococcus*. *BMC Microbiology*. 19(1): 1-14. <https://doi.org/10.1186/S12866-019-1405-Y>.

**Shirling, E.B. and Gottlieb, D. (1972).** Cooperative Description of Type Strains of *Streptomyces*: Additional Descriptions. *International Journal of Systematic and Evolutionary Microbiology*. 22(4): 265-394. <https://doi.org/10.1099/00207713-22-4-265>.

**Shivlata, L. and Satyanarayana, T. (2015).** Thermophilic and alkaliphilic Actinobacteria: Biology and potential applications. *Frontiers in Microbiology*. 6: 156396. <https://doi.org/10.3389/FMICB.2015.01014>.

**Shomura, T.; Yoshida, J.; Amano, S.; Kojima, M.; Inouye, S. and Niida, T. (1979).** studies on actinomycetales producing antibiotics only on agar culture i. screening, taxonomy and morphology-productivity relationship of *Streptomyces halstedii*, strain sf-1993. *The Journal of Antibiotics*. 32(5): 427-435. <https://doi.org/10.7164/ANTIBIOTICS.32.427>.

**Smaoui, S.; Ennouri, K.; Chakchouk-Mtibaa, A.; Sellem, I.; Bouchaala, K.; Karray-Rebai, I. et al. (2018).** Modeling-based optimization approaches for the development of Anti-*Agrobacterium tumefaciens* activity using *Streptomyces* sp. TN71. *Microbial pathogenesis*. 119: 19-27. <https://doi.org/10.1016/j.micpath.2018.04.006>.

**Thom, C. and Raper, K.B. (1945).** A manual of the Aspergilli, Vol. 60. Philadelphia: LWW, 333.

**Tormo, J.R.; García, J.B.; DeAntonio, M.; Feliz, J.; Mira, A.; Díez, M.T. et al. (2003).** A method for the selection of production media for actinomycete strains based on their metabolite HPLC profiles. *Journal of Industrial Microbiology & Biotechnology*. 30(10): 582-588. <https://doi.org/10.1007/S10295-003-0084-7>.

**Vimali, E.; Senthil Kumar, A.; Sakthi Vignesh, N.; Ashokkumar, B.; Dhakshinamoorthy, A.; Udayan, A. et al. (2022).** Enhancement of lipid accumulation in microalga *Desmodesmus* sp. VV2: Response Surface Methodology and Artificial Neural Network modeling for biodiesel production. *Chemosphere*. 293: 133477. <https://doi.org/10.1016/J.CHEMOSPHERE.2021.133477>.

**Wellington, E.M.H. and Cross, T. (1983).** Taxonomy of antibiotic-producing actinomycetes and new approaches for their selective isolation. In: *Progress in industrial microbiology*, Bushell, M.E. (Editor). Elsevier, Amsterdam. pp. 36.

**Wickerhams, L.J. (1951).** Taxonomy of Yeasts. US Department of Agriculture, Washington DC. Technical Bulletin No.1029. 1-56.

**Yi, J.S.; Kim, M.; Kim, S.J. and Kim, B.G. (2015).** Effects of sucrose, phosphate, and calcium carbonate on the production of pikromycin from *Streptomyces venezuelae*. *Journal of Microbiology and Biotechnology*. 25(4): 496-502. <https://doi.org/10.4014/jmb.1409.09009>.